A PERK-miR211 axis suppresses circadian regulators and protein synthesis to promote cancer cell survival

Yiwen Bu[1], **Akihiro Yoshida**[1], **Nilesh Chitnis**[1], **Brian J. Altman**[2], **Feven Tameire**[7], **Amanda Oran**[3], **Victoria Gennaro**[3], **Kent E. Armeson**[4], **Steven McMahon**[3], **Gerald B. Wertheim**[5], **Chi Van Dang**[2], **Davide Ruggero**[6], **Constantinos Koumenis**[7], **Serge Y. Fuchs**[8], and **J. Alan Diehl**[1,9]

[1]Department of Biochemistry and Molecular Biology and Hollings Cancer Center, Medical University of South Carolina, Charleston, SC 29425, USA

[2]Abramson Cancer Center, Perelman School of Medicine, University of Pennsylvania, PA19104, USA

[3]Department of Cancer Biology, Sidney Kimmel Medical College, Thomas Jefferson University, PA19107, USA

[4]Department of Public Health Sciences and Hollings Cancer Center, Medical University of South Carolina, Charleston, SC 29425, USA

[5]Department of Pathology and Laboratory Medicine, Children's Hospital of Philadelphia, PA 19104, USA

[6]Departments of Urology and Cellular and Molecular Pharmacology, Helen Diller Family Comprehensive Cancer Center, University of California, San Francisco, San Francisco, CA 94158, USA

[7]Department of Radiation Oncology, Perelman School of Medicine, University of Pennsylvania, Philadelphia, PA 19104, USA

[8]Department of Biomedical Sciences, School of Veterinary Medicine, Philadelphia, PA 19104, USA

Summary

The Unfolded Protein Response (UPR), is a stress activated signaling pathway that regulates cell proliferation, metabolism and survival. The circadian clock coordinates metabolism and signal transduction with light/dark cycles. We have explored how UPR signaling interfaces with the circadian clock. UPR activation induces a 10h phase shift in circadian oscillations through

---

[9]Corresponding Author: J. Alan Diehl, diehl@musc.edu.

Disclosure of potential conflicts of interest: The authors declare no conflict of interests.

induction of miR-211; miR-211, a PERK inducible micro-RNA, transiently suppresses both Bmal1 and Clock, core circadian regulators. Molecular investigation reveals that miR-211, directly regulates Bmal1 and Clock via distinct mechanisms. While suppression of Bmal1 and Clock have the anticpated impact of expression of select circadian genes, we find that repression of Bmal1 is also essential for UPR-dependent inhibition of protein synthesis and cell adaptation to stresses that disrupt endoplasmic reticulum homeostasis. Our data demonstrate that c-myc-dependent activation of the UPR inhibits Bmal1 in Burkitt's lymphoma thereby suppressing both circadian oscillation and ongoing protein synthesis to facilitate tumor progression.

Keywords

UPR; PERK; Circadian Clock; miR-211; Bmal1; Clock; c-Myc

Introduction

Misfolding within the endoplasmic reticulum (ER) triggers a cellular checkpoint pathway referred to as the Unfolded Protein Response (UPR). The UPR is a signaling pathway composed of three transducers, PERK, Ire1 and ATF6 [1]. Inositol regulated kinase-1 (Ire1) is a signal pass membrane localized protein kinase that also exhibits exonuclease activity[2, 3]. Ire1 regulates expression of numerous ER chaperones through activation of the X-box binding protein 1 (Xbp1) transcription factor [4] and accumulation of Xbp1 is mediated by Ire1-dependent splicing activity [5, 6]. Protein kinase RNA (PKR)-like ER kinase, (PERK), also an ER transmembrane protein kinase, that catalyzes serine 51 phosphorylation on eIF2α resulting in reduced protein synthesis [7–9]. The third signaling components are the transmembrane transcription factors ATF6α/β.

Physiological stresses that induce the UPR include metabolic challenge, viral infection, low oxygen and oncogenic signaling [1]. In the context of such stresses, the UPR functions to determine cell fate by reducing protein synthesis, increasing chaperone expression to increase protein folding capacity, or initiate apoptosis under conditions of ongoing stress and cellular damage that can not be repaired. Because the UPR is frequently engaged during tumor progression, where it facilitates tumor cell survival [10–13], signal transducers such as PERK and Ire1 are potential targets of therapeutic intervention.

While the UPR plays an important role in cell proliferation, metabolism and survival, how it intersects with other signaling pathways that coordinate cell fate decisions remains poorly understood. The circadian clock coordinates gene expression and protein translation with proliferation and metabolism in the context of light/dark cycles. The heterodimeric transcription factor, Bmal1:Clock, is the central regulator of the core and peripheral circadian clock; alterations in Bmal1/Clock or downstream circadian components has been implicated in metabolic disorders[14–16] and tumorigenesis[17, 18]. The UPR also contributes to metabolic homeostasis and tumor cell survival under conditions of micro-environmental and metabolic stress[19] suggesting the potential for cross-talk between these two pathways. In the experiments described herein, we have explored the intersection of the Circadian Clock with

UPR signaling. The ensuing data reveal striking cross-talk which impacts upon both normal and tumor cell survival.

Results

UPR activation disrupts circadian oscillation

To investigate a potential intersection between the UPR and the circadian clock, dexamethasone synchronized U2OS cells expressing a Bmal1 promoter-driven luciferase reporter were exposed to the ER stress inducer, thapsigargin (Tg), and Bmal1-reporter expression was longitudinally assessed using a LumiCycle luminometer[20]. Tg treatment triggered a phase shift in *Bmal1* expression (Fig 1a, *upper panel*) and co-administration of the PERK inhibitor, GSK2606414 [21], suppressed the phase shift (Fig 1a, *lower panel*). Likewise, Bmal1 and Clock protein accumulation was transiently suppressed in a PERK-dependent manner (Fig 1b). IRE1 deletion did not inhibit Bmal1 or Clock loss demonstrating a specific role for PERK (Fig 1c). Similar results were observed in cells challenged with tunicamycin (Tm) or by glucose deprivation (Fig S1a).

To assess UPR-circadian clock cross-talk *in vivo*, livers were collected from 8 week-old wild type (PERK$^{loxp/loxp}$) or knockout (PERK$^{\Delta/\Delta}$) mice[16] at 6-hour intervals following exposure to Tm. Treatment of PERK$^{\Delta/\Delta}$ mice generated discolored livers (Fig S1b) reflective of extensive hepatonecrosis (Fig S1c). Consistent with PERK mediating stress-dependent survival, PERK$^{\Delta/\Delta}$ mice had to be sacrificed within 2 days of Tm treatment, compared to 6-days for PERK$^{loxp/loxp}$ mice (Fig S1d). Tm increased eIF2α phosphorylation and Chop induction in PERK$^{loxp/loxp}$ mice consistent with PERK activation (Fig S1e). Tm exposure triggered a circadian phase shift in *Bmal1* and *Clock* expression in PERK$^{loxp/loxp}$ livers (Fig 1d); oscillation of Bmal1-Clock circadian gene targets was correspondingly shifted (Fig 1e). PERK$^{\Delta/\Delta}$ mice were refractory to Tm-induced phase shift; a reduced amplitude in Bmal1 and Clock mRNA was observed (Fig 1d) reflecting enhanced cytotoxicity to Tm.

We noted that mRNAs encoding UPR signaling components exhibit circadian oscillation consistent with cross talk between these two pathways (Fig 2a). To expand our understanding of physiological UPR/circadian clock cross-talk, we determined whether entrainment to darkness triggers UPR activation. Eight-week old male mice were divided into two groups; one group of mice followed a 12:12 hour light/dark (LD) cycle, while in the second group mice were placed in darkness for 48 hours and switched to normal (DD). Livers were harvested for western blot (Fig 2b) and qPCR analysis (Fig 2c). Consistent with entrainment inducing the UPR, we noted PERK and eIF2α hyper-phosphorylation (compare 0 in Control group with 0 in Darkness group, Fig 2b), increased ATF4 accumulation, and alterations in expression pattern of miR-211, CHOP, PERK, ATF4 (Fig 2c). Accumulation of Bmal1 and Clock also exhibited a delay corresponding with miR-211 expression (Fig 2b). We also determined whether a 12 hour shift in light/dark cycle triggers UPR activation. One group of mice followed a 12:12 hour light/dark cycle (Control group), while in the second group light/dark cycles were reversed (DL Reversed). Livers were harvested from both of the groups beginning at 6h post the initial light shift western blot (Fig 2d) and qPCR analysis (Fig 2e). Consistent with entrainment inducing the UPR, we noted PERK hyper-

phosphorylation, increased p-eIF2α, and ATF4 accumulation. Oscillation of Bmal1 and Clock was also abrogated by the light/dark reversal (Fig 2e).

PERK inducible miR-211 suppresses Bmal1 and Clock

The kinetics of UPR-dependent Bmal1/Clock suppression is analogous to induction of PERK induced miR-211[22] (Fig 3a and Fig 3b) suggesting miR-211 as a plausible link. Consistent with a regulatory interaction, a miR-211 inhibitor (A211), abolished UPR-dependent Bmal1 and Clock suppression (Fig 3c) and restored their circadian oscillation (Fig 3d). We also noted strong induction of miR-211 in mouse livers during entrainment to new light dark cycles (Fig 2c). *Dicer*^{−/−} cells were refractory to ER stress-dependent repression of Bmal1 and Clock (Fig 3e) supporting a role for miRNA-dependent regulation[23]. The induction of miR-211 during entrainment to a new light/dark cycle correlated with increased PERK activity and with reduced CHOP expression, as might be expected from previous work [22]; miR-211 induction also correlated with diminished Bmal1 and Clock expression.

To address the mechanism of miR-211 action, we performed a bioinformatic analysis for potential miR-211 seed matches and noted one for miR-211 in the *Clock* 3′UTR (Fig S2). A luciferase reporter was generated harboring either the wild type 3′UTR of Clock or one with mutated seed sequences. Expression of the Luciferase-Clock reporter was suppressed by miR-211 in a seed-dependent manner (Fig 3f). Additionally, wild type but not the mutant Luciferase-Clock reporter, was responsive to ER stress, while A211 abrogated UPR-dependence (Fig 3g).

No miR-211 seed sequences were identified in the 3′UTR of *Bmal1*; however, 3 high relevance matches are present in the proximal promoter/5′-UTR region (Fig S3a) suggesting the potential for miR-211 to regulate *Bmal1* via RNA-Induced Transcriptional Silencing (RITS)[22]. RITS, unlike canonical cytoplasmic RISC, is nuclear micro-RNA complex that recruits EZH2 to target promoters through rare RNA transcripts with extended 5′ sequences; miRNA-dependent engagement of these transcripts promotes the generation of heterochromatic marks facilitating suppression of transcription[24](Fig S3b). To assess this model of regulation, a Bmal1-luciferase reporter with either a wild type Bmal1 promoter or one containing mutations in miR-211 seed sites was engineered. ER stress reduced expression of the wild type promoter but not a mutant mutations in all potential miR-211 seed sequences (Fig 4a). Mutation of individual sites reduced stress-dependent silencing, but to a lesser degree (Fig 4a). Ectopic expression of miR-211 repressed wild type but not mutant Bmal1-luciferase consistent with direct regulation by miR-211 (Fig 4b).

To address miR-211 regulation of endogenous *Bmal1*, we introduced biotinylated wild type or mutant miR-211[25] into cells. Nuclear extracts were subjected to streptavidin pull-down and Bmal1 nascent mRNA was quantified by qPCR. Wild type but not mutant miR-211, was enriched for Bmal1 nascent RNA with a preference for Seed1 and Seed2 (Fig 4c–e) demonstrating the direct interaction between miR-211 and Bmal1 promoter. Equivalent concentrations of wt and mut miR-211 were present on beads (Fig S3c). Binding specificity was confirmed by assessing interactions with the neighboring gene PTH (Fig S3d) and sequences 1000bp upstream from Seed3 sequences (Fig S3e). Consistent with current

models of RITS, ChIP analysis revealed miR-211-dependent recruitment of Argonaut to Bmal1 (Fig 4f). Enhanced H3K27me3 methylation (Fig 4g), but no H3K9me2 methylation (Fig S3f) was observed. In addition, RNA polymerase II occupancy was reduced by ER stress and miR-211 induction (Fig 4h). Collectively, these data suggest that the UPR modulates circadian oscillation via regulation of *Clock* 3′UTR and *Bmal1* transcription through PERK-dependent induction of miR-211.

MYC suppresses Bmal1 and Clock through engagement of the UPR and miR-211

Burkitt's Lymphoma is associated with chromosomal translocation (t(8;14)(q24;q32)) resulting in c-myc overexpression; high c-myc triggers increased protein synthesis[26, 27], robust UPR[11] and accumulation of miR-211[22]. Since c-myc potently triggers PERK-dependent miR-211 accumulation and can also intersect with circadian machinery[28], we assessed the impact of c-myc and oncogenic ER stress on *Bmal1* and *Clock*. Comparison of normal human Germinal center B (GC B) cells isolated from human tonsils with Burkitt's lymphoma cell lines Raji, Ramos and CA46 revealed high levels of active PERK and undetectable Bmal1 and Clock expression in lymphoma cells (Fig 5a). Reduced Bmal1/Clock was reflective of increased miR-211 expression (Fig 5b). Downstream circadian targets of Bmal1/Clock, (Per1, Per2, Cry1 and Cry2), were also reduced (Fig S4). Expression of A211 in lymphoma cell lines restored expression of Bmal1 and Clock (Fig 5c–d) as did treatment of cells with a PERK small molecule inhibitor GSK2606414 (Fig 5e–f). A211 expression or PERK inhibition also restored circadian oscillation of Bmal1 and Clock in lymphoma cells (Fig 5g–j). Metabolic genes, including *NAMPT*[29], *ODC1*[30] and *UPP2*, exhibit *BMAL1*-dependent circadian oscillations[28]. The rescue of Bmal1/Clock by A211 or through PERK inhibitor increased expression of these metabolic genes (Fig 5k–l) [31]. These data collectively provide support for the role of PERK-miR-211 in mediating the impact of Myc and the UPR on circadian oscillations through regulation of Bmal1 and Clock.

To further address the interconnection of miR-211, circadian gene expression and oncogenic stress, we analyzed murine lymphomas driven by c-myc [32]. Reduced expression of Bmal1 and Clock was noted in all tumors (Fig 6a, Fig S5); this correlated with PERK-dependent phosphorylation of eIF2α (Fig 6a) and miR-211 accumulation (Fig 6b). We subsequently turned to human Burkitt's lymphoma, a tumor where Bmal1 expression is significantly reduced[33] (Fig 6c). We assessed miR-211 versus Bmal1/Clock expression in 5 available cases of human primary lymphoma with a documented c-myc translocation[11]. Bmal1 expression was reduced relative to normal and this negatively correlated with miR-211 expression (miR-211 expression previously reported[22]) in these tumors (Fig 6d)[11, 22].

To address whether the miR-211/Bmal1/Clock relationship is lymphoma specific, we turned to a model of Her2/Neu driven mammary carcinoma. miR-211 expression in murine MMTV-Neu tumors is dependent on the PERK [22]. As with lymphoma, Bmal1 and Clock expression inversely correlates with miR-211 (Fig 6e).

Bmal1 repression contributes to tumor cell survival

The inhibition of Bmal1/Clock by the UPR implies that reduction and the issuant impact Bmal1 and/or Clock regulatory functions are important for cell viability and ultimately for tumor cell survival. We focused on Bmal1 under ER, since the level of Bmal1 repression in tumors was more striking than that of Clock. We addressed Bmal1 contributions to survival through Annexin V staining (acute stress) or clonogenic assay (transient stress and long term survival) in U2OS cells where Bmal1 expression is driven by a heterologous promoter. Enforced Bmal1 expression conferred high sensitivity to ER stress (Fig 7a; Fig S6a). Importantly, enforced Bmal1 expression also suppressed anchorage-independent growth of Burkitt's lymphoma cells (Fig S6b–c), conditions that induce ER stress [34]. *In vivo*, Bmal1 overexpression or A211 significantly suppressed CA46 xenograft tumor growth (Fig 7b–c; Fig S6d–e). Tumors overexpressing wildtype Bmal1 or A211 exhibited high rates of apoptosis and decreased proliferative indeces (Fig S6f, Fig 7d–e). We also examined additional human cancer etiologies by mining online databases to assess the impact of Bmal1 expression on tumor progression. Critically, breast, lung and gastric cancer patients who have higher Bmal1 overexpression showed better overall survival (Fig 7f)[35].

We next determined whether N-myc, like C-myc, regulates Bmal1 through use of N-myc amplified neuroblastoma cell lines; Kelly and NLF. SHEP and SKNAS do not contain N-myc amplicons and served as controls [28]. Kelly and NLF have siginificantly higher miR-211 expression, p-eIF2α activation, and correspondingly low Bmal1 expression (Fig S7a). Use of a small molecule bromodomain inhibitor JQ1[36] to suppress myc transcription, reduced p-eIF2α, miR-211 and increased Bmal1 expression (Fig S7b). In contrast, increasing N-myc expression in SHEP and SKNAS cells, induced miR-211, with a concomitant decrease in Bmal1 (Fig S7c), demonstrating N-myc, also regulates the miR-211/Bmal1 axis. In colon cancer cell line HCT116, cervical cancer cell line HeLa and breast cancer cell line MCF7 we observed that myc knockdown decreased miR-211 levels and rescued Bmal1 expression, while no rescue was observed in H1299 (Fig S7d).

Bmal1 loss is necessary for UPR-dependent repression of protein synthesis

In addition to transcription, Bmal1 also regulates translation initiation through direct association with eIF4F[17]. Since PERK plays an essential role in reducing protein overload during ER stress and myc-driven lymphoma[11] through inhibition of protein synthesis, we investigated whether PERK-miR-211 triggered Bmal1 loss during UPR contributes to global protein translation inhibition. Pulse-label analysis of U2OS cells in which Bmal1 expression was enforced demonstrated Bmal1 overrides UPR-dependent protein translation inhibition in response to ER stress (Fig 8a). Cells that retained Bmal1 did not exhibit significant alterations in S6 ribosomal protein phosphorylation, but maintained hyperphosphorylated 4EBP1 relative to control cells (Fig 8b). Consistently, while eIF4E and eIF4A binding to the m[7]GTP cap was reduced in control cells, enforced Bmal1 expression resulted in modestly increased binding (Fig 8c). Since miR-211 targets Bmal1, we addressed the role of miR-211 in regulating protein translation regulation under ER stress. Expression of A211, which prevents Bmal1 loss (Fig 3c), prevented UPR-dependent protein translation inhibition (Fig 8d).

PERK signaling regulates cell viability under ER stress via modulation of protein translation[14]. We determined whether increased sensitivity to ER stress is a reflection of Bmal1-dependent protein synthesis. Transient exposure to thapsigargin in the presence of cycloheximide (CHX) reduced cell death in U2OS Bmal1 cells (Fig 8e). Previous work demonstrated increased sensitivity of PERK−/− cells to ER stress due to the lacking of protein translational control via p-eIF2α-ATF4 axis[37]. Bmal1 knockdown abrogated ER stress toxicity of PERK−/− cells demonstrating the importance of PERK/miR211 suppression (Fig 8f; S7e).

Since Bmal1 regulates gene transcription and protein synthesis (Fig 8a), we addressed whether Bmal1-dependent regulation of gene transcription versus its impact on protein translation drives differential cell survival under ER stress. We introduced Bmal1S42G (defect in protein translation control[17]) or Bmal1ΔHLH (impaired the DNA binding) into U2OS cells. Annexin V staining revealed that only Bmal1 S42G reduced the ER stress sensitivity (Fig 8g), consistent with Bmal1-mediated protein translation regulation contributing to cell survival under conditions of ER stress. We also noted that the impact of of Bmal1S42G expression on growth of CA46 xenografts was much less than wild type Bmal1 expression (Fig 7b). The capacity of 4-Phenylbutyrate (4-PBA) treatment to reduce apoptosis in CA46 cells engineered to express Bmal1 is consistent with the model wherein enforced Bmal1 expression triggers ER stress (Fig 8h).

Discussion

The UPR was initially identified and characterized as a response to pharmaceutical challenges that perturb the oxidative, pro-folding environment of the ER. The identification of a signaling pathway that coordinates cellular response to such challenge has facilitated investigation of physiological challenges that engage the UPR; challenges that include low oxygen, glucose restriction, metabolic stress and alterations in protein synthesis rates [1]. While our understanding of how the UPR regulates cell fate has increased, there remains a gap in our understanding of cross-talk between the UPR and distinct signaling pathways that respond to or regulate common pathways.

There is a growing appreciation for the capacity of the UPR and circadian machinery to contribute to cell growth and metabolism. Yet, the notion of a coordinated impact through UPR and circadian cross-talk has not been evaluated. This work demonstrates that the UPR directly regulates the core circadian clock. UPR activation in cell culture triggers a 8–10h shift in circadian phase oscillation; this shift is exquisitely dependent upon PERK-eIF2α-ATF4 signaling. Mechanistically, the ATF4 inducible micro-RNA, miR-211, directly suppresses both Bmal1 and Clock. Because miR-211 is a label miRNA under normal conditions [22], Bmal1 and Clock suppression is transient. Cross-talk is not limited to cell culture as activation of the UPR in mice, via pharmacological treatment with tunicamycin also triggers PERK-dependent shifts in circadian oscillation. Importantly, we also note that alterations in the normal light/dark cycle triggers UPR activation, hinting that the UPR may contribute to clock re-entrainment.

The transient loss of Bmal1 has a direct impact on downstream circadian and metabolic gene expression, but also has a direct impact on protein translation. This unanticipated role for Bmal1 in the regulation of protein synthesis has a profound effect on cell survival following pharmacological ER stress and in tumor cells where Bmal1 is silenced as a consequence of PERK signaling.

The initial delay in circadian transcript oscillation will undoubtably contribute to the ultimate tumor progression by virtue of alterations in the coordination of metabolic gene expression. However, the necessity of Bmal1 suppression for reducing protein synthesis will have a more immediate impact. Targeted deletion of PERK in c-myc driven lymphoma results in ER protein overload and tumor cell death [11]. The results described herein suggest that PERK-miR-211 dependent suppression of Bmal1 is an essential aspect of this pathway necessary for progression of c-myc positive lymphoma. As tumors continue to progress and experience ongoing metabolic challenge, alterations in circadian gene expression and metabolic regulation will likely have a more direct contribution to tumor cell survival. Ultimately, the repression of Bmal1 by PERK-induced miR-211 has the remarkable capacity to robustly contribute to cell survival and tumor progression by limiting protein overload.

Methods

Cell culture

Human osteosarcoma U2OS cells (ATCC HTB-96) were purchased in 2014 from American Type Culture Collection (ATCC) and maintained in McCoy's 5a medium (Mediatech Inc) supplemented with 10% of FBS (BenchMark) and 1% of Penicillin-Streptomycin. 293T cells (ATCC CRL-3216) were purchased from ATCC in 2014 and were maintained in DMEM medium (Mediatech Inc) with 10% FBS. Burkitt's lymphoma cell lines CA46 (ATCC CRL-1648), Raji (ATCC CCL-86) and Ramos (ATCC CRL-1596) were purchased from ATCC in 2015 and maintained in RPMI-1640 medium (Mediatech Inc) with 10% FBS and 1% Penicillin-Streptomycin (Gibco). Wild-type and PERK-knockout (KO), IRE-1-knockout (KO) mouse embryo fibroblasts (MEFs) were maintained in DMEM supplemented with 10% FBS, 1% Penicillin-Streptomycin, 2mM glutamine (Gibco), 55 μM β-mercaptoethanol (Gibco) and MEM nonessential amino acids (Gibco). U2OS Bmal1::Luc cells were provided by Dr. John Hogenesch (University of Cincinnati). SKNAS-NmycER cells were provided by Dr. Linda J. Valentijn, University of Amsterdam, Netherlands. In SKNAS-NmycER[38] and SHEP-NmycER cells[39], N-myc protein was induced with 0.5μM 4-hydroxytamoxifen (4OHT, Sigma, H7904).

Plasmids and retroviruses

pBMPC3-Bmal1(mouse) plasmid (#31367) was purchased from Addgene. Bmal1 was subcloned into MSCV-IRES-GFP (MigR1). PCKPC4 Clock (mouse) plasmid was purchased from Addgene (#31366). Plenti-Bmal1(human) and Plenti-Clock (human) were purchased from Applied Biological Materials Inc (MT-h04606, Canada). All mutations/deletions were generated using either the In-Fusion cloning kit (Clontech, Cat 011614) or Cold Fusion cloning kit (Clontech, Cat 011614). Human Bmal1 S42G was mutated from AGC(Serine) to GGC(Glycine) at 42aa. pABpuro-BluF (#46824) was purchased from Addgene. Retroviral

vectors and helper plasmids were co-transfected into 293T cells by lipofectamine (ThermoFisher Scientific, WA). Retroviral supernatants were collected 48–72 hours post transfection. Retroviral infection was mediated by 10μg/ml Polybrene (Millipore #TR-1003-G, Germany). pmiRZip-211 (anti-miR-211 lentiviral construct) was purchased from System Biosciences.

Radiolabeling

U2OS vector and Bmal1 stable cells were treated with Tg 500nM as indicated, deprived of methionine for 30 minutes, and re-fed with medium containing 100 μCi EasyTag EXPRESS ^{35}S (PerkinElmer). Cell lysates were collected, quantified by Bradford assay and resolved by 10% SDS-PAGE. ^{35}S-met incorporation was quantified by ImageQuant software and total protein was quantified by ImageLab software.

Real-time luminescence monitoring

U2OS Bmal1::Luc cells were cultured and treated as described previously[28]. In brief, cells synchronized by dexamethasone were measured by lumicycle luminometer every 10 minutes for at least 4 days in the presence of beetle luciferin in the cell culture medium. The signal was presented as relative light unites (RLU) per second (Actimetrics).

Human subjects

All the human samples were previously described[22], and were obtained with informed consent and IRB approval. Human tonsils were obtained from routine tonsillectomies performed in Philadelphia Children's Hospital (CHOP). Informed consent was obtained from patients. Tissue collection was approved by the hospital ethical committee.

Magnetic cell isolation of human Germinal Center B cells (CD27+CD10+)

Tonsils were placed on ice immediately following surgical removal at Children's Hospital of Philadelphia. After mincing, cells were passed through a 40μm cell strainer. For isolation of germinal center B cells non B- cell populations were first depleted using the B Cell Isolation Kit II, human (130-091-151). Flow-through B cells were then labeled with anti-CD27-PE antibody (130-097-926) and subsequently magnetically labeled with Anti-PE MultiSort MicroBeads according to manufacturer's instructions. Cells not stained with anti- CD27-PE were depleted by magnetic separation on LS columns (130-042-401). Following positive selection, the magnetic beads were removed from the cells by using the Anti-PE MultiSort Kit (130-090-757). CD27 positive cells were then stained with anti-CD10-Biotin antibody (130-114-691) according to manufacturer's instructions. Magnetically labeled CD10 positive cells were isolated after passing through LS columns. All reagents are purchased from Miltenyi Biotec.

Flow cytometric analysis

Apoptosis was quantified using the APC Annexin V Apoptosis Detection Kit (BD Biosciences). FACS was performed on a BD LSRFortessa (BD Biosciences) and analyzed by FlowJo (TreeStar). The detailed procedure was performed according to the manufactururer's instructions. Briefly, single cell suspensions were prepared and washed

with cold PBS then suspend in $1 \times$ Binding buffer at a concentration of 1×10^6 cells/ml. Transfer 100 μl of the solution to a tube and add 5 μl APC Annexin V. Gently rortex the cells incubate for 15 minutes at Room temperature in the dark. Add 400 μl of $1\times$ Binding buffer to each tube and subject to FACS analysis within 1 hr.

miR-211 and anti-miR-211(A211) transfection and analysis

U2OS cells were transfected with control, miR-211 or A211 using lipofectamine 2000 (Invitrogen). For the lymphoma cell lines, transfection was conducted twice due to the low transfection efficiency. miRNA was isolated by using the miReasy mini kit (Qiagen), amplified and reverse transcribed using Taqman reverse transcription kit (Applied biosystems). U6 snRNA and snoRNA202 served as internal controls for human and murine samples, respectively.

Animal husbandry

All animal experiments were conducted within the guidelines with the Animal Care and Use Committee of Medical University of South Carolina. For the circadian measurements, PERK[loxp/loxp] and PEKRΔ/Δ mice were generated as previous described[16]. PERK[loxp/loxp] genotype was confirmed by PCR using Primers Forward 5′-CACTCTGGCTTTCACTCCTCACAG, Reversed 5′-GTCTTACAAAAAGGAGGAAGGTGGAA. CreERT2 genotype was confirmed by PCR using primers Forward 5′-TACACCAAAATTTGCCTGCATTACCGG and Reversed 5′-TTTCCAAGAGTGAACGAACCTGGT. PEKRΔ/Δ mice were generated by intercrossing Cre-ERT2 heterozygous mice with PERK[loxp/loxp]. For PERK deletion, Tamoxifen (T5648, Sigma-Aldrich) was administrated via oral gavage at a dose of 0.20 mg/g of bodyweight/day for 5 consecutive days. The PERK excision was confirmed by genotype PCR using primers F1 5′-CATCCCCATCAGCCTGTTTG, R1 5′-TCTTGGTTGGGTCTGATGAAT, F2 5′-GATGTTCTTGCTGTAGTGGGGG, R2 5′-GGTCAAGGAAGGCAGATAGGAAAG. All the mice participating experiments are eight-week old male. Tunicamycin was dissolved in 150mM sucrose in PBS and administrated intraperitoneally with 1μg/g bodyweight tunicamycin or vehicle. Mouse livers were collected as 6-hour intervals for 36h. Mice were maintained in 12:12 hour light: dark cycles and 24-hour food access. For entrainment experiment, C57BL/6J mice (male, eight-week old) were purchased from Jackson Laboratory. Control group mice were maintained in normal 12:12 hour light:dark cycles and the entrainment group of mice was placed in complete darkness for 48 hours and then shift back to normal cycles as the control grouop mice. The mice livers were collected immediately after the 48 hours darkness, 6-hour interval for 36 hours. For xenograft experiments, 1×10^6 CA46 cells (treated as indicated) were subcutaneously injected into 6-week old SCID mice with 1:1 matrigel[40]. 5 mice each group. Tumor were palpable after 2 weeks. Tumor volume was measured every 2 days and calculated by the following formula V= (L x W x H)/2, L is the tumor length, W is the tumor width and H is the height. Mice were sacrificed 34 days post tumor implantation.

Clonogenic survival assay

Cells were plated at 2×10^3 cells/ 60 mm dish. Cells were exposed to 300nM Thapsigargin for 3 hours and then changed to normal growth medium. Fresh medium was replenished

every 3 days for 2 weeks. Viable colonies were stained with 2ml 0.5% Giemsa (v/v) solution for 10 minutes in room temperature[41].

Immunohistochemistry

Livers were fixed in 4% buffered formalin, dehydrated, embedded in paraffin and subsequently sectioned with a microtome. H&E staining was conducted by Tissue biorepository and research pathology service facility in Medical University of South Carolina. Xenograft tumors were flash frozen in liquid nitrogen and stored in −80°C. Tissue was sectioned at a range 6–8μm, placed on positively charged slides and air dried on bench before fixing. The tissue was fixed by actone in −20°C for 20 minutes, washed by PBS and incubated with 0.3% H_2O_2 for 10 minutes. The tissue was blocked by normal goat serum and incubated with appropriate primary antibody overnight and secondary antibody for 1 hour. Signal was visualized with a Vectastain ABC Elite kit (Vector Laboratories) and a peroxidase substrate kit DAB (Vector Laboratories). Representative fields from each section was presented in the figures. The Ki-67 antibody (ab15580) was purchased from Abcam. Apoptosis was detected by APO-BRDU-IHC (TUNEL) Apoptosis Kit (Novus Biologicals). Methyl green was used for nuclear counterstain.

Western blot

Tissue was snap frozen on dry ice. 3.5 wt/vol lysis buffer was added and homogenized for 30 seconds or until completely homogenized. Lysates were sonicated and put on ice for 30 minutes with vortexing every 5 minutes. Then the lysate was cleared by 2X centrifugation at 25,000 rpm for 20 minutes. Equal concentration of total protein was subjected to western blot as described[42]. Bmal1 antibody (A302-616A) was purchased from Bethyl Laboratories Inc. Clock (D45B10) Rabbit mAb #5157, PERK (C33E10) Rabbit mAb #5683, Chop (L63F7) Mouse mAb #2895, ATF-4 (D4B8) Rabbit mAb #11815, phospho-eIF2α (Ser51) (119A11) Rabbit mAb #3597, Phospho-4E-BP1 (Thr37/46) (236B4) Rabbit mAb #2855, eIF4E Antibody #9742, IRE1α (14C10) Rabbit mAb #3294, eIF4A (F52) Antibody #2425, S6 Ribosomal Protein (5G10) Rabbit mAb #2217, Phospho-p70 S6 Kinase (Thr389) (1A5) Mouse mAb #9206, and c-Myc Antibody #9402, BCL6(D4I2V) Rabbit mAb #14895 were from Cell Signaling Technology. eIF2α antibody was purchased from ThermoFisher Scientific. β-actin Mouse mAb (AC-74) #5316 was purchased from Sigma. Detailed antibody information is available in supplementary Table 2.

Quantitative RT-PCR analysis

Total RNA and microRNA were extracted using the miReasy mini kit (Qiagen). mRNA was Reverse transcribed using iScript[TM] cDNA synthesis kit (Bio-Rad) according to manufacturer's instructions. Quantitative RT-PCR was performed using SsoAdvanced[TM] Universal SYBR Green Supermix (Bio-Rad) and the data were normalized by GAPDH. The primer sequence for qPCR used in this study was in supplementary Table 1.

Chromatin immunoprecipitation assays and Biotin-211 chromatin precipitation

Biotin labeled miR-211 duplexes were generated as previously reported[25]. Wild type miR-211 (5′UUCCCUUUGUCAUCCUUUGCCU3′Biotin) and mutant miR-211

5′UUUGUCGAGUCAUCCUUUGCCU3′Biotin) oligos were synthesized from Integrated DNA Technologies (Iowa, US) and transfected into U2OS cell via lipofectamine 2000 (ThermoFisher Scientific, WA). Chromatin was prepared using the truChIP low cell chromatin shearing kit (Covaris) and sheared 200–700 bp fragments. Immunoprecipitation was performed using IgG, pan-Ago clone 2A8 (MABE56 Millipore), H3K27me3 (ab6002 Abcam), H3K9me2 (ab1220, Abcam), RNA polII (ab817 Abcam, ChIP grade CTD repeats) antibodies with a Quick ChIP Kit (Imgenex)[22, 32]. Primers used for ChIP assays are in supplementary table 2.

m⁷GTP immunoprecipitation

Cells were lysed in EBC buffer (50 mmol/L Tris, pH 8.0, 120 mmol/L NaCl, 1 mmol/L EDTA, 0.5% NP40) containing complete and PhosStop (1 tablet/10ml, Roche). 1mg lysates were incubated with 40μl of pre-washed m⁷GTP beads (Creative Biolabs) overnight in 4°C. Bound proteins were resolved by SDS-PAGE and visualized by western blot.

Statistics and Reproducibility

All western blot and $^{S}35$ cooperation assay shown here were all successfully repeated at least three times. qPCR was performed three independent times. Mean ± SD were presented. Statistical significance was determined by the two-tailed Student's t test using Prism Graphpad or Excel. P<0.05 was considered statistically significant. The correlation of Bmal1/miR-211 and Clock/miR-211 in human tumor and mice tumors were performed by Spearman's correlation in R.

Data availability

Previously published Burkitt's lymphoma data that have been reanalyzed here are available under GEO accession code GSE2350 [Reference 33]. Data and statistical methods are available in www.Oncomine.org (Reporter ID: 36896_s_at). Source data for Figure 1–8 and Supplementary Figures S1, S3, S6 and S7 have been provided as Supplementary Table 3. All other data supporting the findings of this study are available from the corresponding author on reasonable request.

Supplementary Material

Refer to Web version on PubMed Central for supplementary material.

Acknowledgments

References

1. Diehl JA, Fuchs SY, Koumenis C. The cell biology of the unfolded protein response. Gastroenterology. 2011; 141:38–41. 41 e31–32. [PubMed: 21620842]

2. Tirasophon W, Welihinda AA, Kaufman RJ. A stress response pathway from the endoplasmic reticulum to the nucleus requires a novel bifunctional protein kinase/endoribonuclease (Ire1p) in mammalian cells. Genes Dev. 1998; 12:1812–1824. [PubMed: 9637683]

3. Yoshida H, Haze K, Yanagi H, Yura T, Mori K. Identification of the cis-acting endoplasmic reticulum stress response element responsible for transcriptional induction of mammalian glucose-regulated proteins. Involvement of basic leucine zipper transcription factors. The Journal of biological chemistry. 1998; 273:33741–33749. [PubMed: 9837962]

4. Lee AH, Iwakoshi NN, Glimcher LH. XBP-1 regulates a subset of endoplasmic reticulum resident chaperone genes in the unfolded protein response. Mol Cell Biol. 2003; 23:7448–7459. [PubMed: 14559994]

5. Calfon M, et al. IRE1 couples endoplasmic reticulum load to secretory capacity by processing the XBP-1 mRNA. Nature. 2002; 415:92–96. [PubMed: 11780124]

6. Yoshida H, Matsui T, Yamamoto A, Okada T, Mori K. XBP1 mRNA is induced by ATF6 and spliced by IRE1 in response to ER stress to produce a highly active transcription factor. Cell. 2001; 107:881–891. [PubMed: 11779464]

7. Shi Y, et al. Identification and characterization of pancreatic eukaryotic initiation factor 2 alpha-subunit kinase, PEK, involved in translational control. Mol Cell Biol. 1998; 18:7499–7509. [PubMed: 9819435]

8. Harding HP, Zhang Y, Ron D. Protein translation and folding are coupled by an endoplasmic-reticulum-resident kinase. Nature. 1999; 397:271–274. [PubMed: 9930704]

9. Pytel D, Majsterek I, Diehl JA. Tumor progression and the different faces of the PERK kinase. Oncogene. 2015

10. Bobrovnikova-Marjon E, et al. PERK promotes cancer cell proliferation and tumor growth by limiting oxidative DNA damage. Oncogene. 2010; 29:3881–3895. [PubMed: 20453876]

11. Hart LS, et al. ER stress-mediated autophagy promotes Myc-dependent transformation and tumor growth. The Journal of clinical investigation. 2012; 122:4621–4634. [PubMed: 23143306]

12. Pytel D, et al. PERK Is a Haploinsufficient Tumor Suppressor: Gene Dose Determines Tumor-Suppressive Versus Tumor Promoting Properties of PERK in Melanoma. PLoS genetics. 2016; 12:e1006518. [PubMed: 27977682]

13. Bhattacharya S, et al. Anti-tumorigenic effects of Type 1 interferon are subdued by integrated stress responses. Oncogene. 2013; 32:4214–4221. [PubMed: 23045272]

14. Harding HP, Zhang Y, Bertolotti A, Zeng H, Ron D. Perk is essential for translational regulation and cell survival during the unfolded protein response. Mol Cell. 2000; 5:897–904. [PubMed: 10882126]

15. Zhang P, et al. The PERK eukaryotic initiation factor 2 alpha kinase is required for the development of the skeletal system, postnatal growth, and the function and viability of the pancreas. Mol Cell Biol. 2002; 22:3864–3874. [PubMed: 11997520]

16. Gao Y, et al. PERK Is Required in the Adult Pancreas and Is Essential for Maintenance of Glucose Homeostasis. Mol Cell Biol. 2012; 32:5129–5139. [PubMed: 23071091]

17. Lipton JO, et al. The Circadian Protein BMAL1 Regulates Translation in Response to S6K1-Mediated Phosphorylation. Cell. 2015; 161:1138–1151. [PubMed: 25981667]

18. Bass J, Takahashi JS. Circadian integration of metabolism and energetics. Science. 2010; 330:1349–1354. [PubMed: 21127246]

19. Bu Y, Diehl JA. PERK Integrates Oncogenic Signaling and Cell Survival During Cancer Development. Journal of cellular physiology. 2016

20. Baggs JE, et al. Network features of the mammalian circadian clock. PLoS biology. 2009; 7:e52. [PubMed: 19278294]

21. Axten JM, et al. Discovery of 7-methyl-5-(1-{[3-(trifluoromethyl)phenyl]acetyl}-2,3-dihydro-1H-indol-5-yl)-7H-p yrrolo[2,3-d]pyrimidin-4-amine (GSK2606414), a potent and selective first-in-

class inhibitor of protein kinase R (PKR)-like endoplasmic reticulum kinase (PERK). J Med Chem. 2012; 55:7193–7207. [PubMed: 22827572]

22. Chitnis NS, et al. miR-211 is a prosurvival microRNA that regulates chop expression in a PERK-dependent manner. Molecular cell. 2012; 48:353–364. [PubMed: 23022383]

23. Harfe BD, McManus MT, Mansfield JH, Hornstein E, Tabin CJ. The RNaseIII enzyme Dicer is required for morphogenesis but not patterning of the vertebrate limb. Proceedings of the National Academy of Sciences of the United States of America. 2005; 102:10898–10903. [PubMed: 16040801]

24. Verdel A, et al. RNAi-mediated targeting of heterochromatin by the RITS complex. Science. 2004; 303:672–676. [PubMed: 14704433]

25. Orom UA, Lund AH. Isolation of microRNA targets using biotinylated synthetic microRNAs. Methods (San Diego, Calif). 2007; 43:162–165.

26. Barna M, et al. Suppression of Myc oncogenic activity by ribosomal protein haploinsufficiency. Nature. 2008; 456:971–975. [PubMed: 19011615]

27. Ruggero D. The role of Myc-induced protein synthesis in cancer. Cancer Res. 2009; 69:8839–8843. [PubMed: 19934336]

28. Altman BJ, et al. MYC Disrupts the Circadian Clock and Metabolism in Cancer Cells. Cell metabolism. 2015

29. Garten A, et al. Physiological and pathophysiological roles of NAMPT and NAD metabolism. Nat Rev Endocrinol. 2015; 11:535–546. [PubMed: 26215259]

30. Atwood A, et al. Cell-autonomous circadian clock of hepatocytes drives rhythms in transcription and polyamine synthesis. Proceedings of the National Academy of Sciences of the United States of America. 2011; 108:18560–18565. [PubMed: 22042857]

31. Eckel-Mahan KL, et al. Reprogramming of the circadian clock by nutritional challenge. Cell. 2013; 155:1464–1478. [PubMed: 24360271]

32. Li Y, et al. PRMT5 is required for lymphomagenesis triggered by multiple oncogenic drivers. Cancer Discov. 2015; 5:288–303. [PubMed: 25582697]

33. Basso K, et al. Reverse engineering of regulatory networks in human B cells. Nature genetics. 2005; 37:382–390. [PubMed: 15778709]

34. Avivar-Valderas A, et al. Regulation of autophagy during ECM detachment is linked to a selective inhibition of mTORC1 by PERK. Oncogene. 2012

35. Gyorffy B, Surowiak P, Budczies J, Lanczky A. Online survival analysis software to assess the prognostic value of biomarkers using transcriptomic data in non-small-cell lung cancer. PloS one. 2013; 8:e82241. [PubMed: 24367507]

36. Delmore JE, et al. BET bromodomain inhibition as a therapeutic strategy to target c-Myc. Cell. 2011; 146:904–917. [PubMed: 21889194]

37. Belinsky MG, Chen ZS, Shchaveleva I, Zeng H, Kruh GD. Characterization of the drug resistance and transport properties of multidrug resistance protein 6 (MRP6, ABCC6). Cancer research. 2002; 62:6172–6177. [PubMed: 12414644]

38. Valentijn LJ, et al. Inhibition of a new differentiation pathway in neuroblastoma by copy number defects of N-myc, Cdc42, and nm23 genes. Cancer research. 2005; 65:3136–3145. [PubMed: 15833843]

39. Ushmorov A, et al. N-myc augments death and attenuates protective effects of Bcl-2 in trophically stressed neuroblastoma cells. Oncogene. 2008; 27:3424–3434. [PubMed: 18193081]

40. Yoshida A, Lee EK, Diehl JA. Induction of Therapeutic Senescence in Vemurafenib-Resistant Melanoma by Extended Inhibition of CDK4/6. Cancer Res. 2016; 76:2990–3002. [PubMed: 26988987]

41. Xu Z, et al. miR-216b regulation of c-Jun mediates GADD153/CHOP-dependent apoptosis. Nat Commun. 2016; 7:11422. [PubMed: 27173017]

42. Aggarwal P, et al. Nuclear cyclin D1/CDK4 kinase regulates CUL4 expression and triggers neoplastic growth via activation of the PRMT5 methyltransferase. Cancer Cell. 2010; 18:329–340. [PubMed: 20951943]
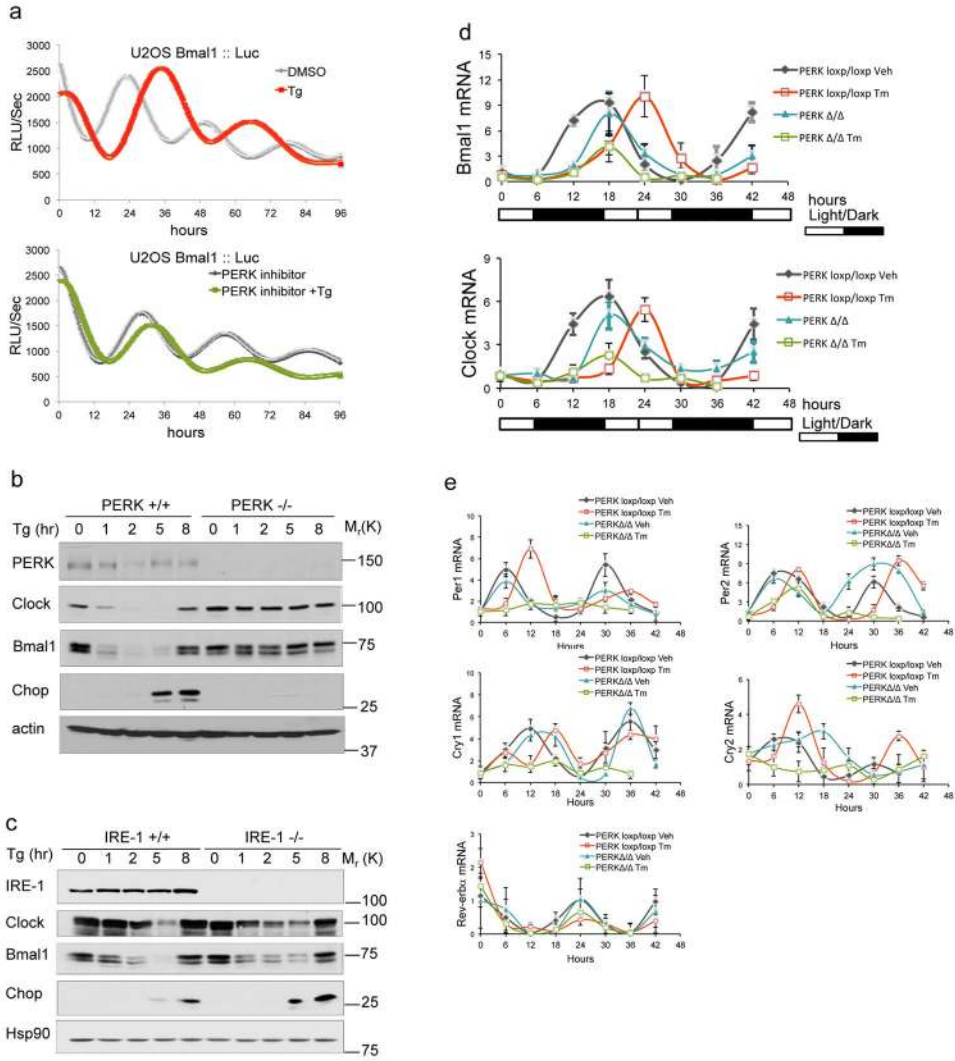
Figure 1. PERK-dependent regulation of circadian oscillation

(a) *Upper panel*: Dexamethasone-synchronized U2OS Bmal1: Luc cells were exposed to thapsigargin (Tg) or unchallenged. Bmal1 promoter activity luminescence was continuously sampled (every 10 minutes) in a LumiCycle luminometer. *Lower panel:* Cells treated as above following 1μM GSK2606414 pretreatment for 1h. Data are representative for n= 3 biologically independent experiments. Source data are available in supplementary Table 3. **(b)** Cell lysates collected from wild type (PERK+/+) or PERK knockout (PERK−/−) MEFs were treated with 0.5uM Tg as indicated. Representative western blots are provided from n=3 biologically independent experiments. **(c)** Cell lysates from wild type or IRE-1 knockout MEFs treated with 0.5mM thapsigargin (Tg) as indicated hours were subjected to western analysis with the indicated antibodies. Data are representative for n=3 biologically independent experiments. **(d–e)** Mice were randomly grouped for vehicle or 1μg/g tunicamycin treatment. Livers were collected every 6 hours for qPCR. White and black boxes indicate the light or dark in the mouse facility. Data represent Mean ± SD from n = 5 mice in each group. Source data are available in supplementary Table 3.
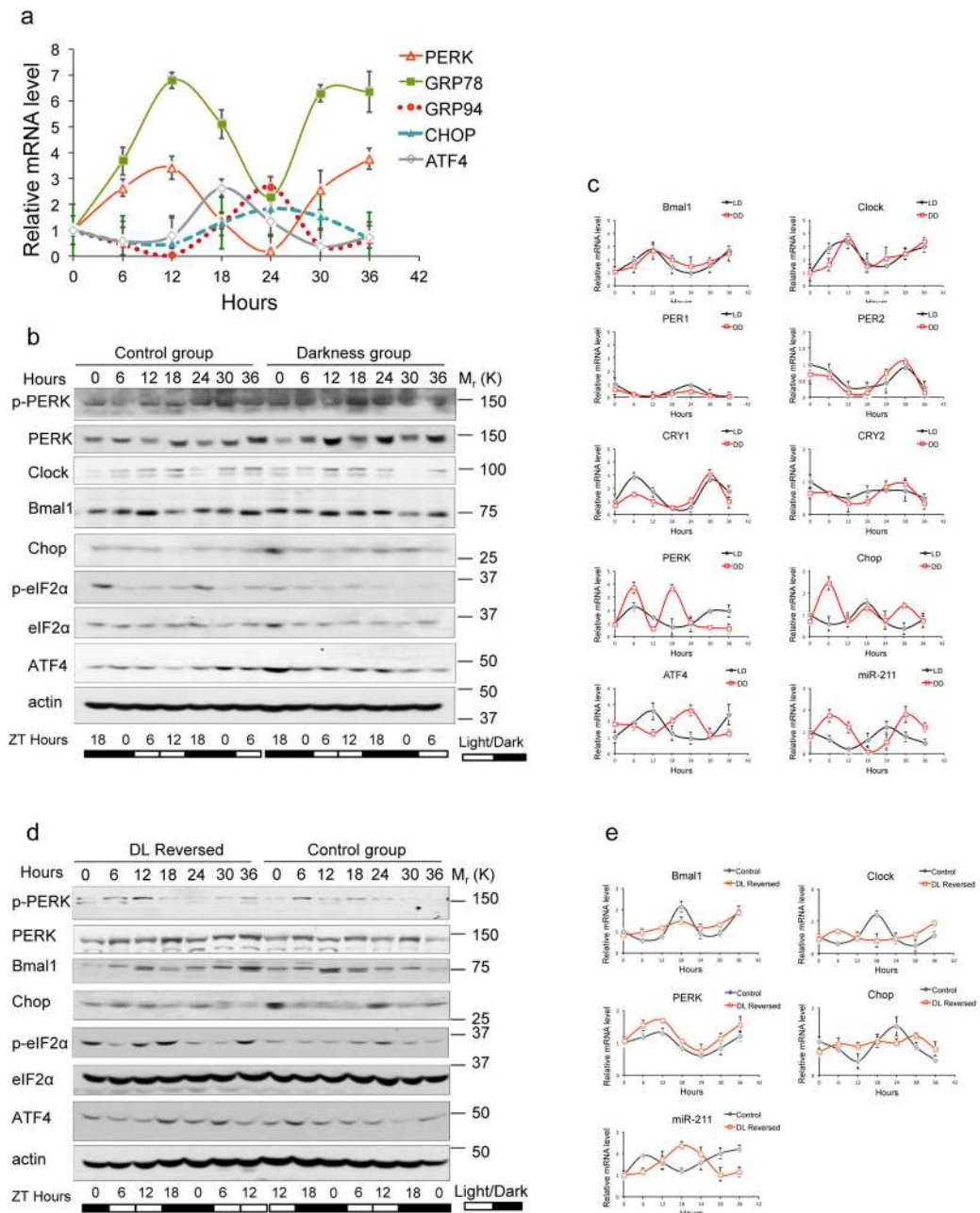
Figure 2. Light/dark reversal triggers the UPR

(**a**) UPR components are expressed in a circadian oscillating manner in mouse livers. Data are Mean ± SD from n=5 mice in each group. (**b–c**) Eight-week old male wild type C57BL/6 mice were randomly divided into 2 groups. Control mice follow the regular 12hr: 12hr light/dark cycles and free access to food (control group). Darkness groups were placed in darkness for 48 hours. Mouse livers were collected every 6 hours for 36 hours. The corresponding Zeitgeber hours (ZT hours) are indicated at the bottom. Light and dark bars represent light and dark, respectively. Protein was isolated for western blot (b). The representative image was shown from n=3 mice per group. RNA was isolated for qPCR in

(c). Data were Mean ± SD from n=3 mice per time point per group. (**d–e**) Wild type C57BL/6 mice were randomly divided into 2 groups. Control mice follow the regular 12hr: 12hr light/dark cycles (control group). In light/dark reversed mice (DL Reversed), light/dark cycles were shifted by 12h. Mouse livers were collected every 6 hours. 0h indicates 6h post the initial light/dark shift. Protein was isolated for western blot in (d). RNA was isolated for qPCR in (e). Data represent Mean ± SD from n=3 mice per time point per group. Source data are available in supplementary Table 3.
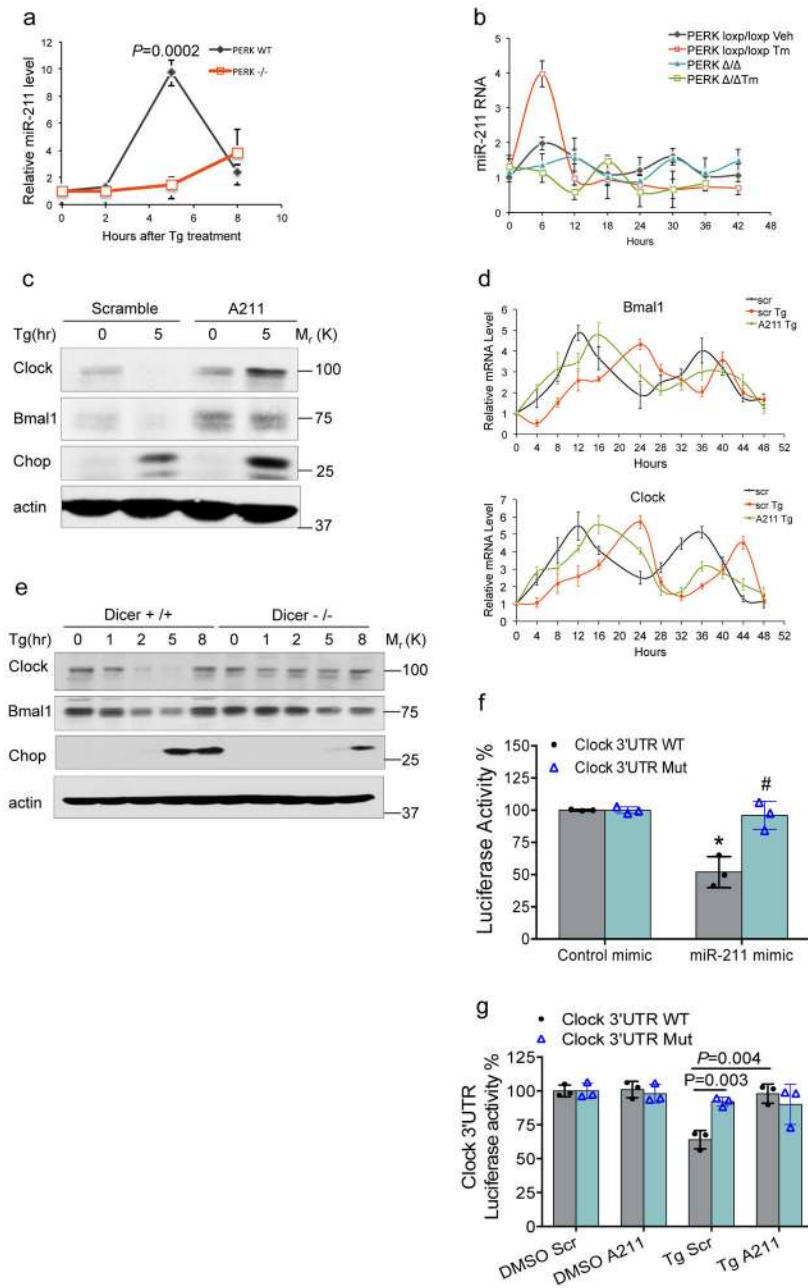
Figure 3. miR-211 directly regulates Clock

(a) miR-211 accumulation in U2OS cells treated with 500nM thapsigargin. Data represent Mean ± SD from n=3 biologically independent experiments, comparing PERK+/+ vs. PERK −/− in the same time point (two-tailed Student's t-test.). **(b)** miR-211 was assessed by qPCR from n=5 mice at each timepoint per group, liver samples are from Fig 1d. **(c)** Cell lysates prepared from U2OS cells transfected with scrambled microRNA or A211 for 48 hours, and treated with thapsigargin for 5 hours were analyzed by immunoblot. Blots representative of n=3 biolgocially independent experiments are provided. **(d)** U2OS cells transfected with scrambled control or A211 were synchronized with 0.1uM dexamethasone and treated with or without 500nM Tg. RNA was collected every 4 hours for 48h for qPCR. Data represent

Mean ± SD from n=3 biologically independent experiments. (**e**) Wild type and Dicer−/−
MEFs were treated with 500nM thapsigargin (Tg) for indicated hours. Cell lysates were
collected for western blot analysis. Blots representative of n=3 biolgocially independent
experiments are provided. (**f**) U2OS cells were transfected with Luciferase-Clock 3′UTR
wild-type or miR-211 site mutant reporter constructs along with Renilla-Luc as an internal
control. Luciferase activity was measured 48h post transfection. Data represent Mean ± SD
(n=3 biologically independent experiments; two-tailed Student's t-test). * *P*=0.002 control
mimic vs miR-211 mimic in Clock 3′UTR wildtype constructs. # *P*=0.009 Clock 3′UTR
wildtype vs. Clock 3′UTR mutant in miR-211 mimic group. (**g**) Luciferase-Clock 3′UTR
wild-type or mutant were introduced into U2OS cells along with scrambled microRNA or
A211. Cells were challenge with Tg for 5h and luciferase activity was measured and
normalized to Renilla. Data represent Mean ± SD (n=3 biologically independent
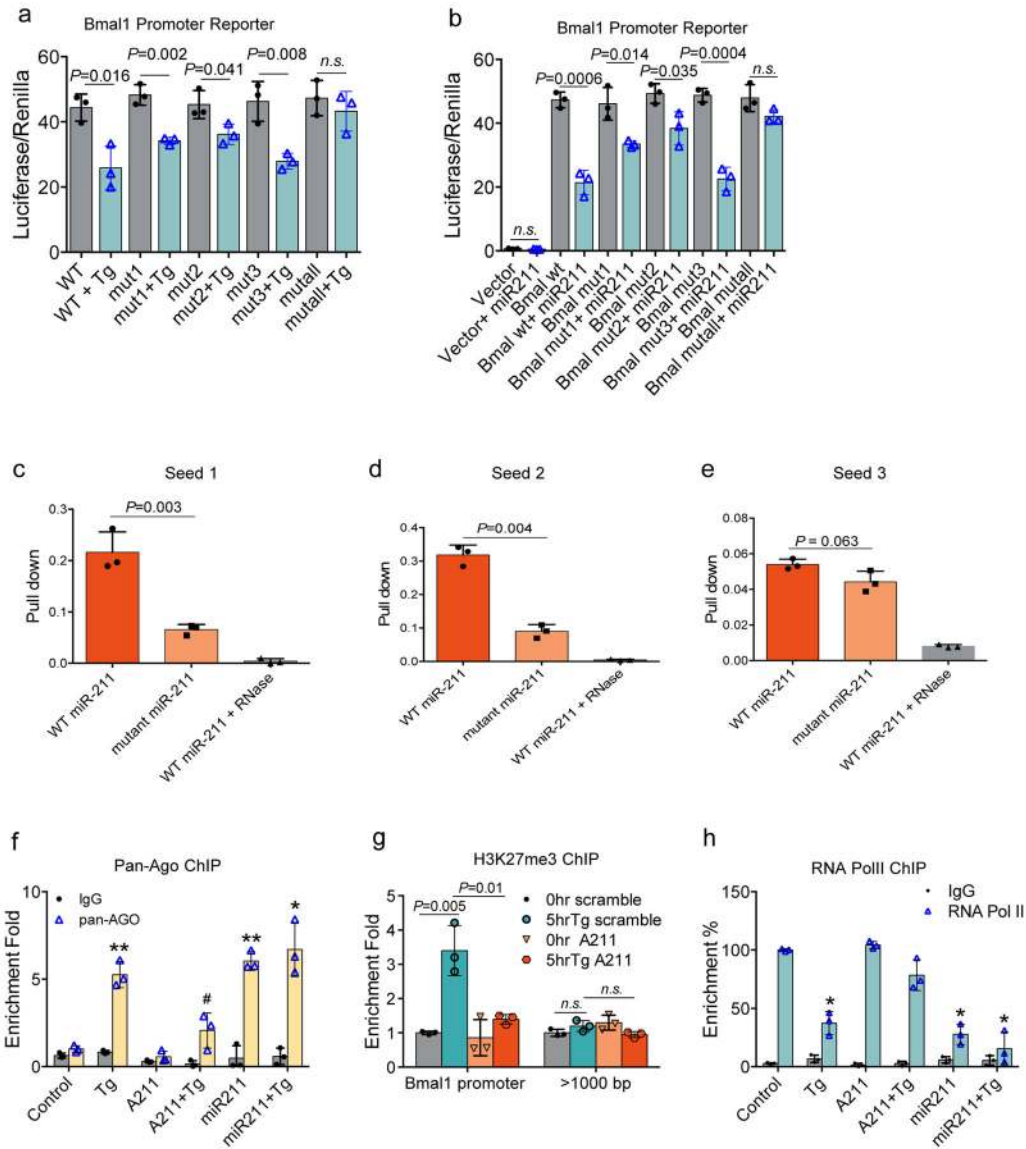experiments; two-tailed Student's t-test). Source data are available in supplementary Table 3.

Figure 4. miR-211 directly targets Bmal1 5′UTR

(**a**) U2OS cells transfected with either wild type or mutant Bmal1-luc promoter reporter constructs were treated with or without Tg. Luciferase activity was normalized to Renilla. Data represent Mean ± SD from n=3 biologically independent experiments. n.s.: not significant. Statistical analysis was performed by two-tail Student's t-test. (**b**) Wild type and mutant Bmal1 promoter luciferase constructs were co-transfected with miR-211 into U2OS cells. Luciferase was measured and normalized to Renilla. Data represent Mean ± SD from n=3 biologically independent experiments. Statistical significance was analyzed by two-tailed Student's t-test. n.s.: not significant. (**c–e**) Biotin-labeled wild type or mutant miR-211 pull down of different regions of Bmal1 promoter RNA. RNA:RNA duplexes were analyzed by qPCR. Data represent Mean ± SD from n=3 biologically independent experiments. Statistical analysis was performed by two-tailed Student's t-test. (**f**) miR-211 or A211 were introduced into U2OS cells and cells were treated with or without Tg. Occupancy of

Argonaut proteins on the Bmal1 promoter was determined by ChIP using a pan-Ago antibody. Data represent Mean ± SD from n=3 biologically independent experiments (Two-tailed Student's t-test). * *P*=0.003 compare to control in AGO group. ** P <0.001 compare to control in AGO group. # P=0.012 compare to Tg in AGO group. Source data are available in supplementary table 3. **(g)** H3K27me3 ChIP for Bmal1 in U2OS cells transfected with A211 and treated with Tg. Data represent Mean ± SD n=3 biologically independent assays. *n.s.*: not significant. Statistical analysis was performed by two-tailed Student's t-test. **(h)** RNA polymerase II ChIP of the Bmal1 promoter. Data represent Mean ± SD n=3 biologically independent assays (two-tailed Student's t-test). *p <0.001 compare with control in RNA polII group. Source data are available in supplementary Table 3.
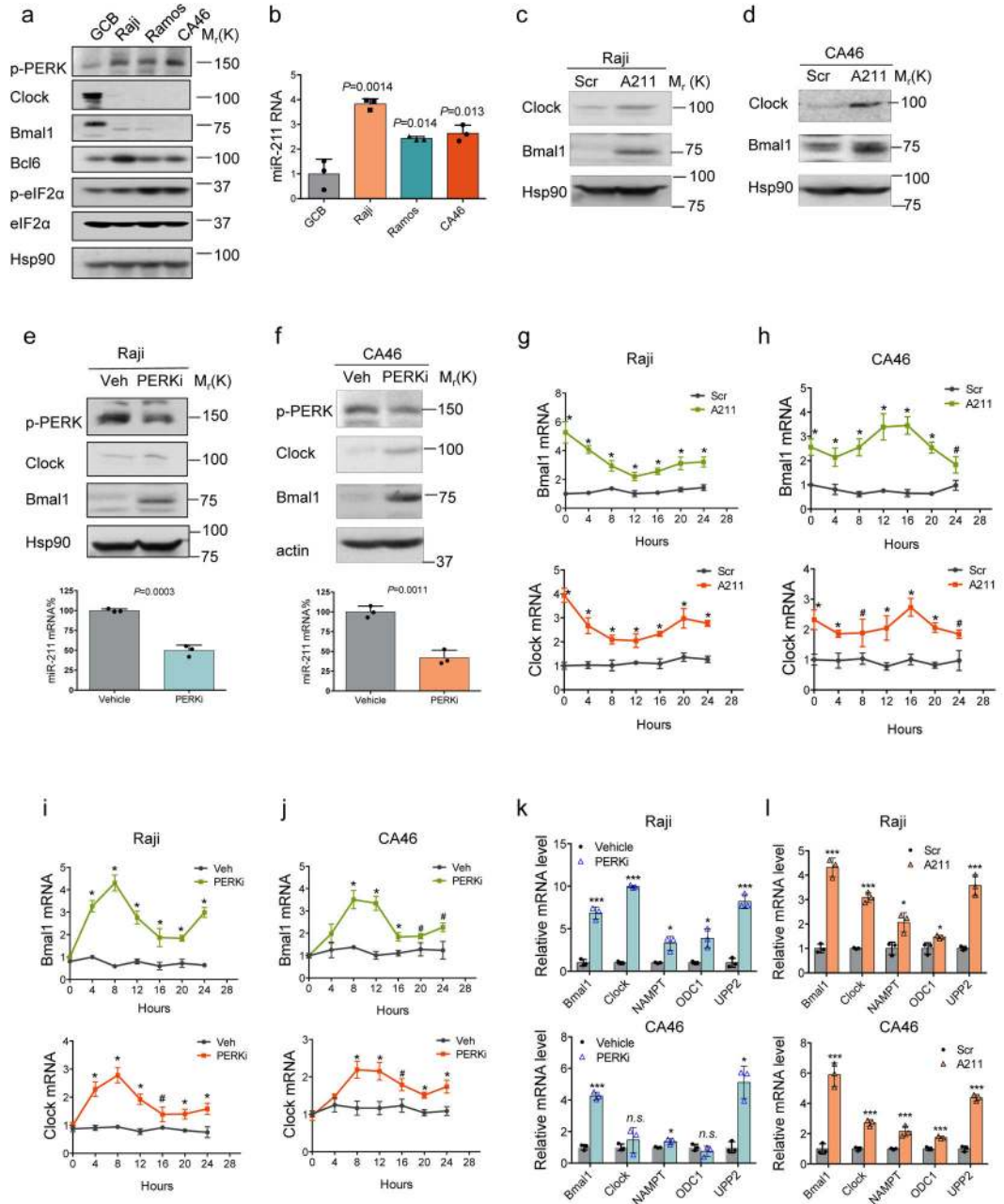
Figure 5. Antagonizing miR-211 restores circadian oscillation
(a) Representative Western blot images and **(b)** qPCR of germinal center B cells (GCB), Raji, Ramos and CA46. Data represent Mean ± SD from n=3 biologically independent measurements. Statistical analysis was performed by two-tailed Student's t-test, comparing to GCB cells. Lysates from **(c)** Raji and **(d)** CA46 cells transfected with scrambled microRNA or A211were analyzed by western blot. Blots are representative of n=3 biolgocially independent experiments are provided. **(e)** Raji and **(f)** CA46 cells were treated with the PERK inhibitor (PERKi; GSK2606414) and subjected to western blot or qPCR. Blots representative of n=3 biolgocially independent experiments are provided. qPCR Data

represent Mean ± SD (n=3 biologically independent measurements). Significance was detemined by two-tailed Student's t-test (95% confidence interval). **(g)** Raji cells **(h)** CA46 cells were transfected with scrambled or A211, synchronized by serum shock and then collected at 4h intervals. Bmal1 and Clock mRNA were assessed by qPCR. Data are Mean ± SD for n=3 biologically independent experiments. *p <0.01, # p<0.05 compared to scramble groups at each time point. Significance was detemined by two-tailed Student's t-test (95% confidence interval). (**i**) Raji cells (**j**) CA46 cells were treated with 1 µM GSK2606414 and cells were collected for qPCR. Data represent Mean ± SD for n=3 biologically independent experiments. Statistical analysis was calculated by two-tailed Student's t-test. * *P*<0.01, # *P*<0.05 compared to Vehicle treatment in at the same time point. Source data and precise p value are available in supplementary Table 3. (**k–l**) PERK inhibition (PERKi) or anti-miR-211 (A211) restores circadian and metabolic gene expression in Burkitt's lymphoma cell lines. Data represent Mean ± SD for n=3 biologically independent experiments. Statistical analysis was calculated by two-tailed Student's t-test. *** P <0.001; * P <0.05. Source data and precise p value are available in supplementary Table 3.
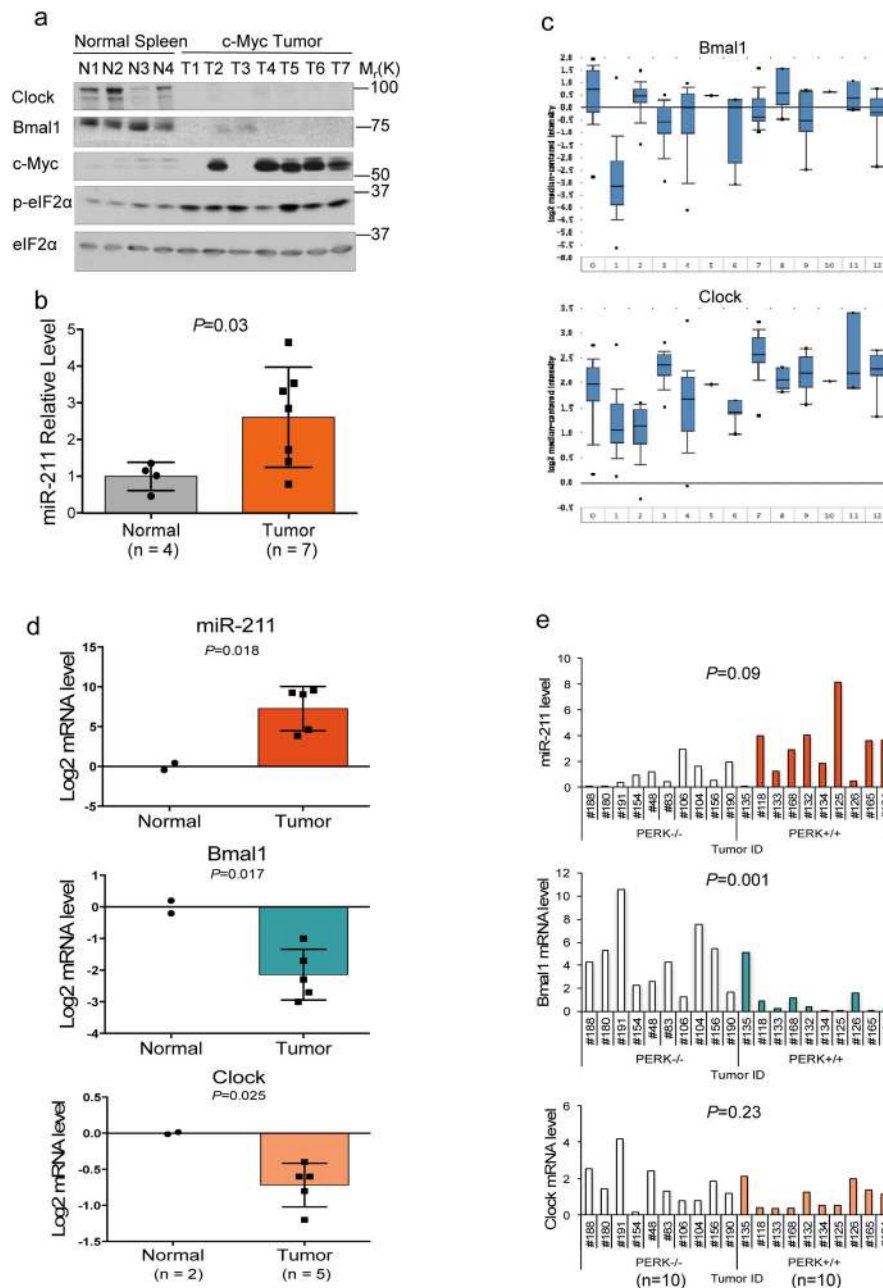
Figure 6. Bmal1 is lost in myc-driven tumors

(**a**) Lymphomas [21] generated by c-Myc expression were analyzed by western blot and (**b**) by qPCR. Representative blots are provided from n=3 biological independent measures. *P*=0.03 for myc-drivn tumor compared to normal samples (95% confidence interval); Statistical analysis was performd by two-sided Two-sample t-test. (**c**) Bmal1 mRNA levels exclusively low in Burkitt's lymphoma. Data and statistical methods are available in www.Oncomine.org (Reporter ID: 36896_s_at){Basso, 2005 #478}. Individual plots for each sample are available in supplementary Table 3. The GEO accession is GSE2350. 0: control (n=58 samples); 1: Burkitt's Lymphoma (n=127); 2: Centroblastic Lymphoma

(n=28); 3: Chronic Lymphocytic Leukemia (n=34); 4: Diffuse Large B-Cell Lymphoma (n=41); 5: Embryonal Rhabdomyosarcoma (n=1); 6: Follicular Lymphoma (n=6); 7: Hairy Cell Leukemia (n=16); 8: Hodgkin's Lymphoma (n=4); 9: Mantle Cell Lymphoma (n=8); 10: Multiple Myeloma (n=1); 11. Plasma Cell Leukemia (n=3); 12: Primary Effusion Lymphoma (n=9). * $p<0.05$ compared to the control samples. **(d)** qPCR analysis of primary human B lymphocytes isolated from normal donors (n=2) and lymphomas from patients with confirmed translocation of c-myc (n=5). miR-211 levels in each sample were previously reported [10]. Data represent Mean ± SD. P value indicates Tumor vs Normal by two-tailed Student's t-test (95% confidence interval). The correlation between Bmal1 and miR-211 rho =−0.29, p=0.56; The correlation between Clock and miR-211 rho=−0.53, p=0.22, calculated by Spearman's Correlation calculated by R. **(e)** miR-211 induction and circadian gene expression are dependent on PERK in mouse MMTV-neu driven breast cancer mouse model. MMTV-neu PERK$^{+/+}$ and MMTV-neu PERK$^{-/-}$ tumors were collected and analyzed by qPCR for the circadian gene mRNA and miR-211. *P* value indicates the gene level comparing PERK$^{+/+}$ and PERK$^{-/-}$ by Two-sample t-test. Spearman correlation between miR-211 and Bmal1: Rho = −0.75, *P*=0.0001; Spearman's correlation between miR-211 and Clock in those tumors: Rho = −0.59, *P*=0.006.
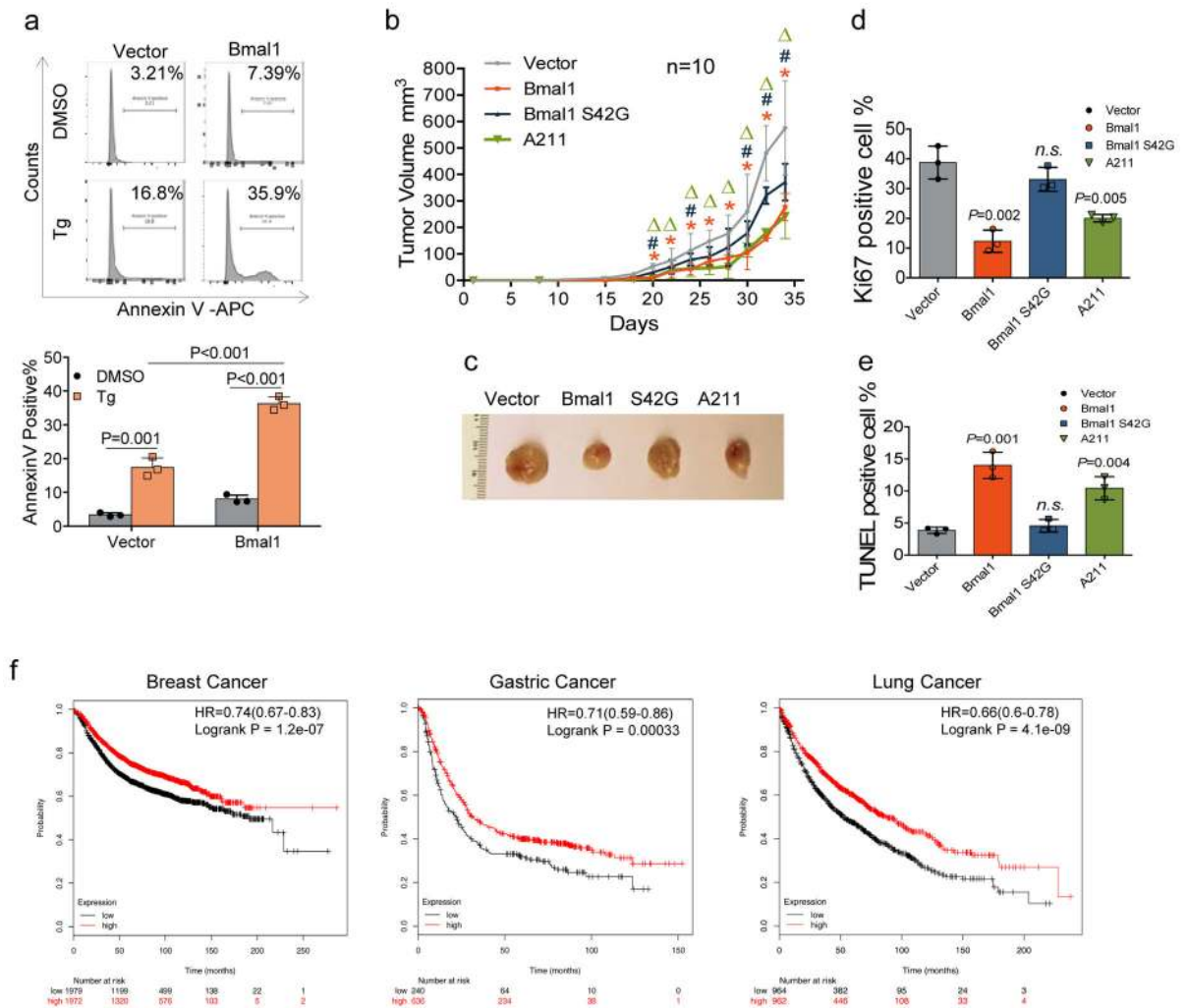
Figure 7. Bmal1 loss is critical for cell survival following ER stress

(a) Parental U2OS-vector or U2OS-Bmal1 cells were treated with 500nM Tg for 72h and apoptosis was quantified by Annexin V. Representative images from n=3 biologically independent experiments and FACS analysis(*upper panel*) are provided. Quantification in barchat represents Mean ± SD from n=3 biologically independent experiments (*lower panel*). Two-tailed Student's t-test. **(b)** CA46 cells were infected with either vector, Bmal1 wild type, Bmal1 S42G or A211 and transplanted into female SCID mice. Data represent Mean ± SD from n=10 tumors in each group. Tumor size was recorded every other day. *p<0.05 compare Bmal1 vs Vector, # p<0.05 compare Bmal1 vs Bmal1 S42G, Δp<0.05 compare A211 vs Vector. Statistical anlaysis was performed by two-tail Student's t-test. The source data and precise p value are available in the supplementary table 3. (**c**) Representative tumor images from each group. (**d–e**) Quantification of immunohistological analysis of the tumor sections. Ki-67(d); TUNEL assay(e). Quantification was assessed from n=3 different tumor slides (two-tailed Student's t-test). n.s.: not significant. **(f)** Bmal1 high expression confers breast cancer, lung cancer and gastric cancer patients better survival. Kaplan-Meier plots assessing impact of Bmal1 expression on survival of breast, lung and gastric cancer patients. Log-rank P value and hazard ratios (HRs; 95% confidence interval in parentheses)

are shown in the bottom. The plots were generated by online tool in kmplot.com. Source data are available in supplementary Table 3.
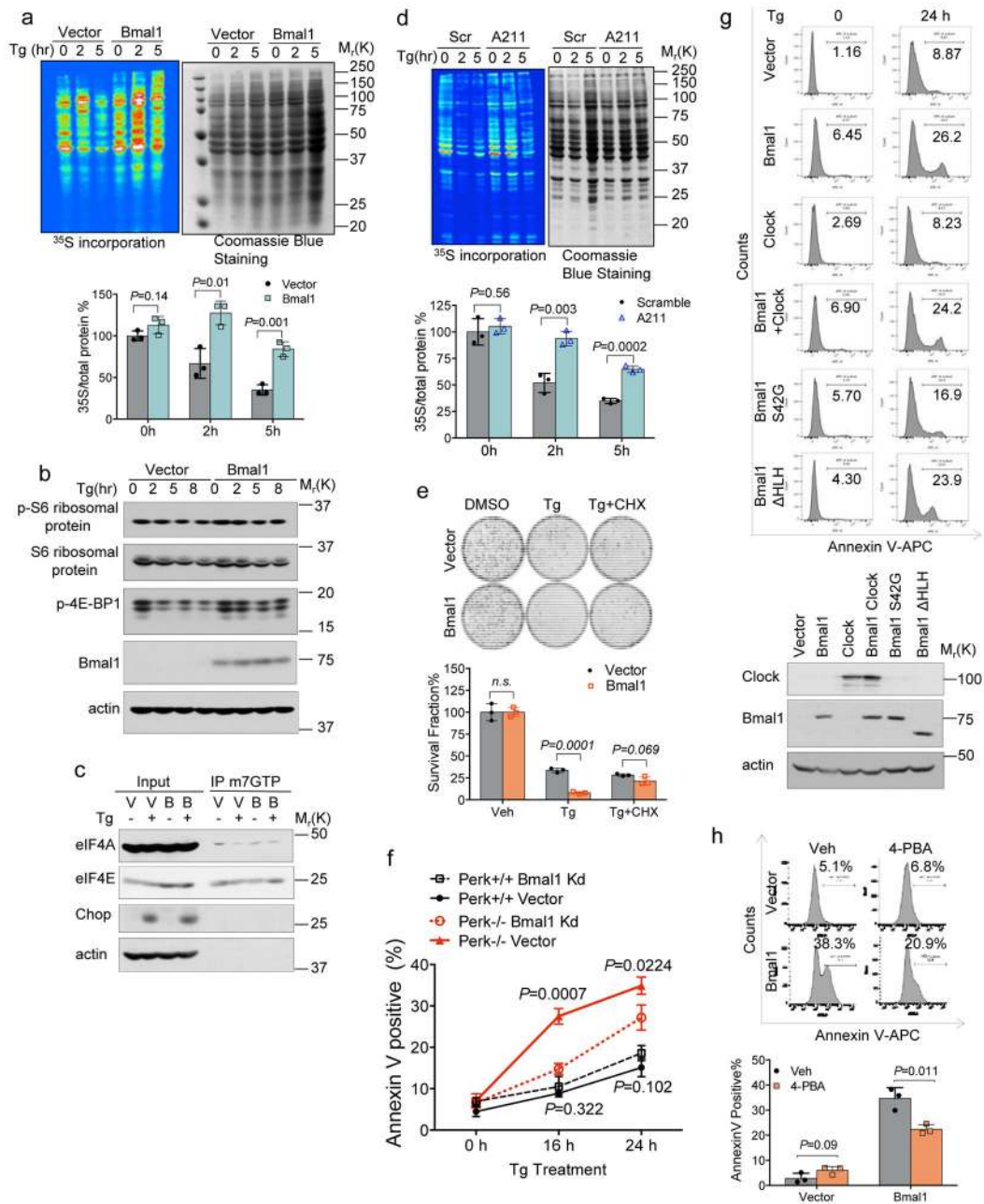
Figure 8. Bmal1 loss is critical for PERK-dependent inhibition of protein synthesis

(**a**) ^{35}S incorporation in U2OS-vector or U2OS-Bmal1 cells following Tg. Autoradiograms were normalized to total protein. Representative images from n=3 independent experiments are provided. Bar chart; Mean ± SD from n=3 experiments. Statistical analysis was performd by two-tailed Student's t-test (95% confidence interval). (**b**) Lysates from U2OS-vector or U2OS-Bmal1 cells treated with Tg. Western blots are representative of n=3 independent experiments. (**c**) Lysates from U2OS vector or U2OS-Bmal1cells treated with Tg were subjected to m[7]GTP pull-down. V = vector only; B = Bmal1 overexpressing cells. Representative blots are provided from n=3 independent experiments. (**d**) ^{35}S incorporation in control or U2OS-miR-211 cells as indicated. Autoradiograms were normalized to total

protein. Representative images are provided from n=3 biologically independent experiments. Bar chart; Mean ± SD from n=3 biologically independent experiments and statistical analysis was performd by two-tailed Student's t-test (95% confidence interval). **(e)** U2OS vector or U2OS Bmal1 cells were treated with Tg (300nM) alone or Tg+cycloheximide for 3h, refed with fresh medium and colonies quantified at 2 weeks. Image is representative of 3 independent experiments (*upper panel*). Value represents Mean ± SD from n=3 independent experiements (*lower panel*). Statistical analysis was performed by two-tailed Student's t-test, comparing vector and Bmal1 cells in each group. n.s. not significant. **(f)** Bmal1 was knocked down, cells were treated with Tg and apoptosis was quantified. Mean ± SD from n=3 independent observations. **(g)** U2OS cells expressing vector, Bmal1, Clock, Bmal1+Clock, Bmal1S42G or Bmal1ΔHLH were treated with Tg for 0 or 24 hours. Apoptosis was assessed by Annexin V staining (*upper panel*); Bmal1 and Clock expression assessed by immunoblot (*lower panel*). Representative data are provided from n=3 independent experiments. **(h)** *Upper panel*: Cells were treated with Vehicle (Veh) or 4-PBA (5mM) for 24 hours, stained with Annexin V and apoptosis quantified by FACS. Representative image from three independent experiments. *Lower panel*: Mean ± SD from three independent experiments. *P* value indicates the comparison between Veh vs. 4-PBA treated cells (95% confidence interval). Statistical analysis was performed by two-tailed Student's t-test. The source data are available in the supplementary table 3.